JOURNAL OF GEOPHYSICAL RESEARCH, VOL. 113, A10308, doi:10.1029/2008JA013208, 2008

DEMETER observations of an intense upgoing column of ELF/VLF radiation excited by the HAARP HF heater

D. Piddyachiy,[1] U. S. Inan,[1] T. F. Bell,[1] N. G. Lehtinen,[1] and M. Parrot[2]

Received 26 March 2008; revised 28 July 2008; accepted 3 September 2008; published 23 October 2008.

[1] DEMETER spacecraft observations of ELF signals generated by the recently upgraded High-Frequency Active Auroral Research Program (HAARP) HF facility (3.6 MW) reveal three distinctive regions characterizing upgoing ELF waves. These regions are classified by signal intensity and the minimum lateral distance d between the magnetic footprint of the satellite at 75-km altitude (D layer) and the point at 75-km altitude immediately above HAARP where the source is located. The first large region within $d \simeq 900$ km contains waves which propagate in the Earth-ionosphere waveguide and then leak upward to the spacecraft. The second region of $d \simeq 200-300$ km contains waves propagating to the spacecraft from the ionospheric source region without reflection from the ground. The third region contains waves of very high intensity ($E \simeq 350$ μV/m, $B \simeq 20$ pT) within a narrow cylindrical column of $\sim$10–20 km radius, also observed once before on the ISIS 1 spacecraft. The observed intense columnar radiation is consistent with predictions of a recent full-wave model of ELF radiation from HF-heater-produced ionospheric source currents.

Citation: Piddyachiy, D., U. S. Inan, T. F. Bell, N. G. Lehtinen, and M. Parrot (2008), DEMETER observations of an intense upgoing column of ELF/VLF radiation excited by the HAARP HF heater, *J. Geophys. Res.*, *113*, A10308, doi:10.1029/2008JA013208.

1. Introduction

[2] ELF signals are known to be generated via modulated HF heating of the lower ionospheric D region within which naturally occurring ionospheric currents flow [*Getmantsev et al.*, 1974; *Moore et al.*, 2006, and references therein]. The presence of the ionosphere not only enables the generation of ELF waves but also determines the propagation characteristics of these waves. For ground-based observations at distant points, the ELF signals propagate within the Earth-ionosphere waveguide, and exhibit maxima near multiples of 2 kHz which are attributed to waveguide resonance effects [*Stubbe et al.*, 1982; *Rietveld et al.*, 1989]. As the ELF waves propagate within the Earth-ionosphere waveguide, some wave energy penetrates through the ionosphere into the overlying magnetosphere. Previous in situ measurements of HF-heating-generated ELF/VLF signals have included those at low altitudes observing signals propagating from the source to the satellite without reflection from the ground [*James et al.*, 1984] and those at laterally distant locations, involving propagation in the Earth-ionosphere waveguide and continuous penetration through the ionosphere upward to higher altitudes [*Platino et al.*, 2006]. However, there exist relatively few spacecraft observations of ELF waves generated via HF heating, with many remaining unknowns. One important parameter concerns the amount of ELF power propagating upward from the heated region. In the work of *James et al.* [1984] the E field measured aboard the ISIS 1 spacecraft at $\sim$1200 km altitude was sustained at the level of 200 μV/m for 525 Hz, 1575 Hz and 1725 Hz in the close region of $d \leq 50$ km (where d is defined as the lateral distance at the altitude of the source between magnetic footprint of the satellite at this altitude and the center of the source). It even reached the value of 2.6 mV/m for 525 Hz at one data point, which was disregarded by the authors as a possible measurement anomaly. The effective source currents deduced from ISIS data were 1 to 2 orders of magnitude larger than currents calculated from ground-based measurements for the same event. On the other hand, in the work of *Kimura et al.* [1991] the results of *James et al.* [1984] were questioned. Measurements on the Akebono satellite over HIPAS [*Kimura et al.*, 1991] showed maximum fields of $E \simeq 15$ μV/m and $B \simeq 0.25$ pT for 2.5 kHz signal. Maximum fields in Akebono measurements over Tromso HF heater [*Kimura et al.*, 1994] were found to be $E \simeq 4$ μV/m and $B \simeq 2$ pT at 2.5 kHz. For these fields in space lower than the ISIS 1 measurements, the effective source currents were calculated to be consistent with ground observations.

[3] In this paper we present observations of relatively high amplitude ELF E and B fields measured on the DEMETER satellite when its footprint was in close proximity of the High-Frequency Active Auroral Research Program (HAARP) HF heated spot together with simultaneous measurements on the ground. Our observations

[1]STAR Laboratory, Stanford University, Stanford, California, USA.
[2]Laboratoire de Physique et Chimie de l'Environnement, CNRS, Orléans, France.

0148-0227/08/2008JA013208$09.00

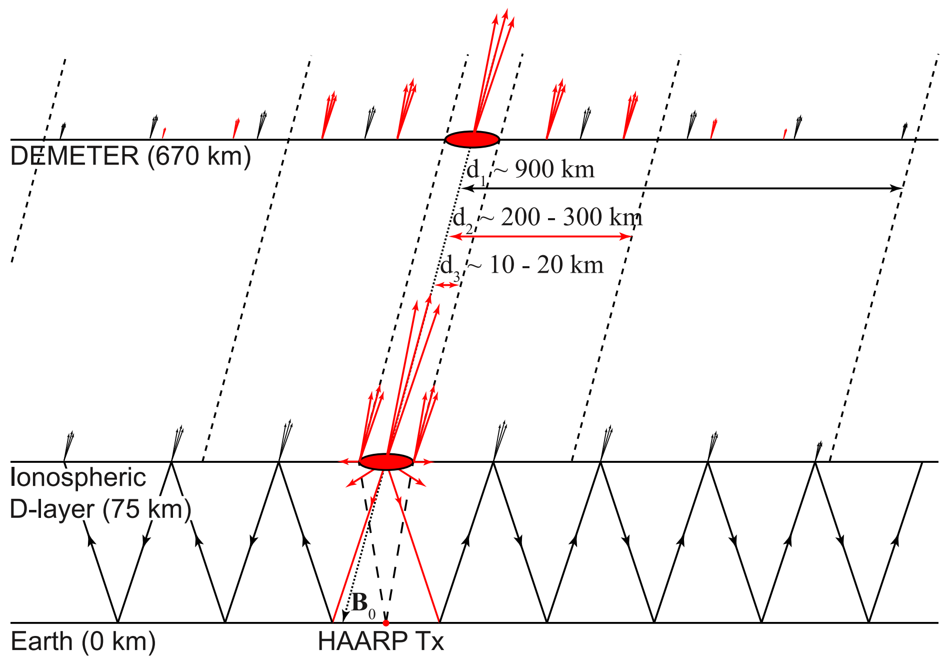

Figure 1. Experimental setup and schematic results of observations. Three observed regions of ELF field intensity are shown by dotted lines. Arrow bunches schematically indicate Poynting flux direction and magnitude of HAARP-generated ELF waves. Red arrows represent waves coming directly from the source in *D* layer, while black arrows represent waves reflected from the ground. Please note Figure 1 is not to scale.

generally support the observations of *James et al.* [1984] and thus provide evidence for the existence of a high power cylindrical column of ELF radiation propagating upward along the magnetic field line emanating from the source region (i.e., the heated region).

[4] Our observations also provide information on the total size of the ELF illumination region at the satellite altitude and the manner by which HAARP-generated ELF waves reach different parts of this region. We show that the signal can be detected at lateral distances of at least $d \simeq 900$ km, which may be the furthest lateral distance of HF-heater-generated ELF signals ever observed in space. We also find that the boundary at $d \simeq 200$ km between ELF waves propagating directly from the source and those reflected from the ground is clearly distinguished by a sharp amplitude variation of the fields as observed along the satellite track. The general features of our observations are consistent with recently developed full-wave model [*Lehtinen and Inan*, 2008] of ELF radiation produced by HF heater modulation of electrojet currents.

2. Description of Experiment

[5] The ELF/VLF signals generated in the *D* region of the ionosphere by the HAARP HF ionospheric heater are observed on the DEMETER spacecraft as it passes through the region above HAARP (Figure 1), and also by ground-based VLF receivers near HAARP.

[6] The High Frequency (HF) ionospheric heater used herein [*Kennedy and Kossey*, 2002] is a component of the High-Frequency Active Auroral Research Program (HAARP) facility located near Gakona, Alaska, at geographic position of 62.39°N, 145.15°W, corresponding to L $\simeq$ 4.9. The recently upgraded HAARP HF heater consists of a 180-element phased array antenna fed by distributed transmitters at each antenna element with total maximum continuous power of 3.6 MW. HAARP can operate at HF ranging from 2.8 MHz to 10 MHz, and in the experiments described below it was used at 3.25 MHz to provide maximum heating in the *D* region of the ionosphere [*James et al.*, 1984]. At this frequency the net radiated power is 3.2 MW, the antenna array gain is 21 dB, the effective radiated power (ERP) at the center of the beam is 407 MW, and the full-width half-power beam width in the north–south plane is 17.2° and in the east–west plane is 13.5°. In our experiments the HF beam was directed vertically upward and the HF carrier was modulated with two types of ELF/VLF modulation formats as shown in Table 1.

[7] Both formats use sine wave amplitude modulation of the HF waves, polarized in the extraordinary (X) mode to provide the maximum ELF radiated power [*Kapustin et al.*, 1977; *Stubbe et al.*, 1982]. The precise ELF/VLF frequencies were chosen to avoid interference from power line harmonics [*Helliwell et al.*, 1975]. The first pattern represents a rich set of different ELF/VLF signal types and frequencies to test the effectiveness of ELF/VLF generation and upward propagation into space. The second pattern is a relatively simple repetition of two frequencies intended for the study of the spatial variation of signal as the DEMETER satellite moves above HAARP.

[8] DEMETER is a low-earth-orbit satellite with an altitude of approximately 670 km, inclination of 98.3° and horizontal velocity of about 7.6 km/s [*Parrot*, 2006]. For HAARP campaigns DEMETER operated in the burst mode,

Table 1. Formats of Modulation Transmitted by HAARP

First Pattern		Second Pattern	
Duration, s	$f(t)$,[a] Hz	Duration, s	$f(t)$,[a] Hz
1	510	1	2011
1	820	1	1111
1	1225	2	0[b]
1	1510	1	2011
1	1875	1	1111
1	2125	2	0[b]
1	2375	1	2011
1	3165	1	1111
1	3365	2	0[b]
1	4365	1	2011
10	$200t + 20\sin(10t) + 400$	1	1111
5	$500t + 500$	2	0[b]
1	5 chirps[c] starting at 1000 Hz	1	2011
1	1225	1	1111
1	5 chirps[c] starting at 1500 Hz	2	$1000t$
1	1875		
1	5 chirps[c] starting at 2000 Hz		
10	$100t + 30\sin(3.33t) + 1100$		
10	$200(t - 40) + 500$		
10	$200t + 40\sin(5t) + 400$		

[a]In each interval t starts with 0 s.
[b]No modulation is imposed. HF power is maintained at 50% level to equalize it with sine wave modulation.
[c]Duration of each chirp is 0.2 s. It is described as $f(t) = f_0 + 1000\sqrt{5t}$, where f_0 of the first chirp in a sequence is the starting frequency in the table which decreases by 70 Hz for each next chirp.

in which broadband waveforms of 3 components of both E and B fields up to 1.25 kHz and one component of each field up to 20 kHz are recorded. In this work one horizontal component of E and one horizontal component of B are used in most cases except for analysis of wave parameters when we use all 6 components. The used component of E is perpendicular to the orbital plane while the component of B is inclined 45° to this component and to the orbital plane. Electron and ion densities were measured by a Langmuir probe and thermal plasma analyzer. We also use ELF/VLF (~100 Hz to 40 kHz) data from the Stanford ground-based receiver in Chistochina, located 37 km to the northeast from HAARP at 62.6°N, 144.6°W. For this latest round of HAARP experiments, DEMETER burst recordings were specially extended beyond the normal termination at invariant latitude of 65°.

[9] In addition to the HAARP-generated ELF signals, signals from the HF ionospheric heater at the HIgh Power Auroral Stimulation (HIPAS) observatory situated about 300 km to the north from the HAARP at 64.87°N, 146.84°W were also coincidentally observed in one case. HIPAS has a maximum ERP of 80 MW at either 2.85 MHz or 4.53 MHz [*Kimura et al.*, 1991].

3. Observations

[10] The first test operations of the full power HAARP HF heater were carried out during 24 February to 4 March 2007. During this period 8 DEMETER passes over HAARP and 3 passes over its conjugate region were scheduled to record in the burst mode. In all passes DEMETER's magnetic footprint at 75-km altitude was within $d \leq 300$ km of the heated spot or its geomagnetic conjugate at 75-km altitude. HAARP ELF/VLF signals were detected on 6 passes over HAARP but none in the conjugate region. This detection rate was much higher than in previous experiments with DEMETER when the pre-upgraded HAARP signal was seen in only 3 out of 12 passes [*Platino et al.*, 2006] and also higher than in other satellite experiments with HF heaters. Part of the lack of success of the early observations can be attributed to the fact that DEMETER observations were then terminated at the invariant latitude of 65°, owing to spacecraft maneuvers. Although the increase of the HAARP radiated power level and favorable geomagnetic conditions may also have played the role, we note that the highest Kp during the campaign was just 4^+ and highest hourly AE was equal to 589 nT. In this work we concentrate on two passes on 1 March and 26 February 2007 which were well positioned with respect to HAARP, with the ELF signals being detected over large regions.

[11] The 1 March 2007 pass was one of the closest satellite passes near an ELF modulated HF ionospheric heater. Figure 2 contains a map with the satellite footprint at an altitude of 75 km, and HAARP and HIPAS HF heater locations. Concentric circles represent the distance of 50, 100, 200, 300, and 400 km from the corresponding heater. The closest distances to HAARP and HIPAS were respectively $d \simeq 50$ km and $d \simeq 60$ km. The three panels show spectrograms for the period from 07:03:50 UT to 07:05:30 UT which corresponds to the satellite projection shown on the map. The top panel is a spectrogram of east–west horizontal component of the B field measured at Chistochina. The middle and the bottom panels are the spectrograms of horizontal components of E and B fields respectively from DEMETER. At this time Kp was 3^- and AE was 171 nT. The ELF modulation pattern was the first one (Table 1) for this pass. The signal at Chistochina exhibits no significant changes in time, and generally a high signal to noise ratio enables the recognition of the entire pattern transmitted, with higher harmonics also visible in some cases. During this DEMETER pass, HIPAS was also coincidentally operating, producing long (10, 20 or 30 s) tones around 1 and 2 kHz.

[12] Examination of the frequency-time ramps and pulses of different frequency indicates that as the frequency increases from 0.5 to 2 kHz the power of the signal on the ground increases by about one order of magnitude. The ramps are short enough so that any natural variations in the auroral electrojet strength can be ignored and the observed variation can be attributed purely to the dependence of ELF generation and propagation on frequency. The signal strength on DEMETER first of all depends on the distance of the satellite from the magnetic field line of the heater. As the satellite moves northward, it first passes a region of high field near HAARP and then a similar one near HIPAS. The signal to noise ratio on DEMETER for the E field is higher than for the B field in this case, so that the signal in the E field spectrograms is visible over a larger region. The dependence of the signal strength on distance in this type of observation is intertwined with the dependence of generation efficiency on the ELF frequency. Figure 3 shows in detail the most interesting part of the pass when DEMETER footprint at 75-km altitude is in close proximity to the HAARP heated spot. The first three panels are magnified versions of the spectrograms in the Figure 2, while the last three panels represent linear plots of field amplitudes

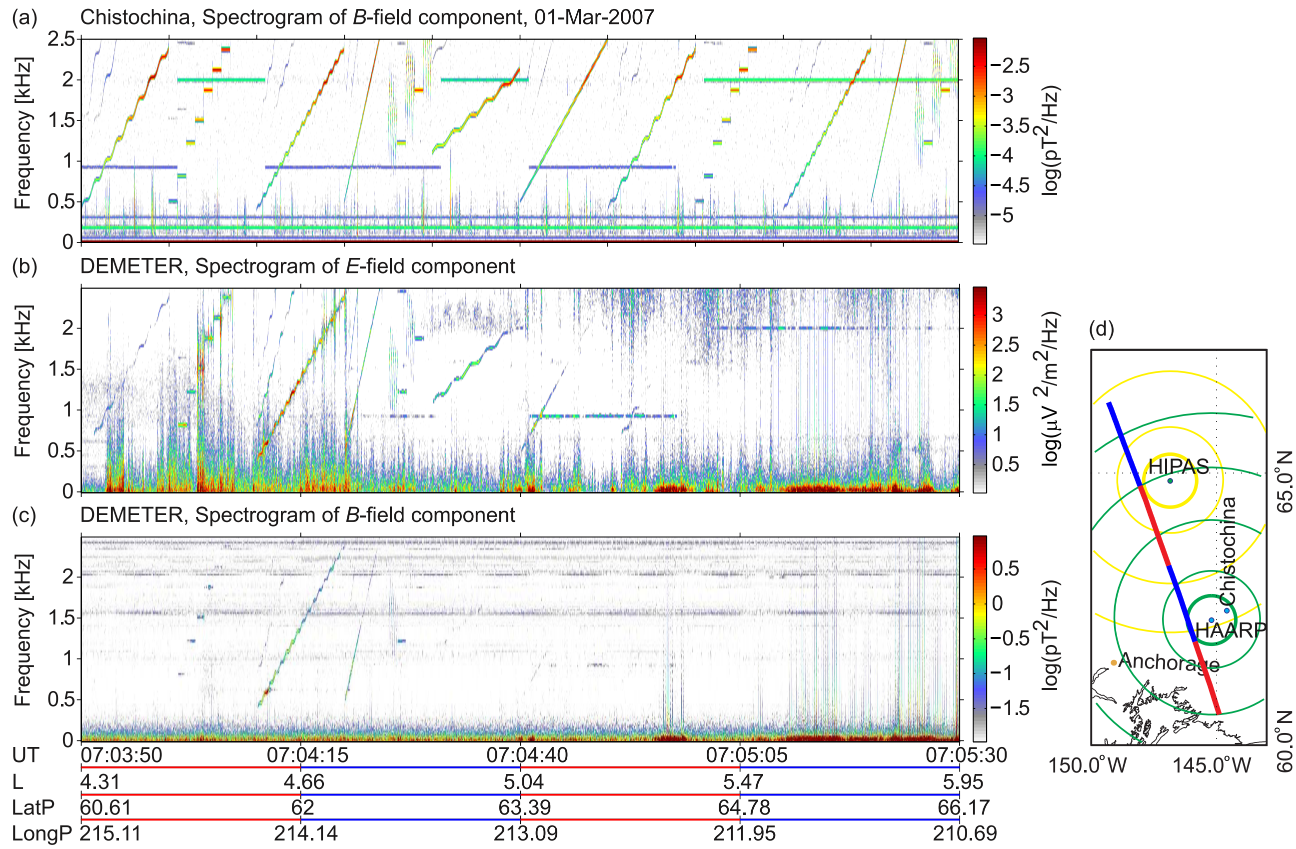

Figure 2. Simultaneous spectrograms of the ELF field during DEMETER pass on 1 March 2007. (a) East–west horizontal B field component on the ground in Chistochina. (b) A horizontal component of E field on DEMETER. (c) A horizontal component of B field on DEMETER. (d) A map showing projection along the Earth's magnetic field lines of the corresponding satellite pass onto the horizontal plane at the altitude of the source (75 km) together with the position of HAARP and HIPAS. The frequency resolution of FFT is 19.5 Hz.

calculated along the main harmonic of the snake ramp. We can see that the trend of the frequency dependence observed on the satellite is generally opposite to that seen in ground-based data, and that the amplitude in space is more variable. The most interesting features are two peaks in E field and corresponding high and low peaks in B field amplitudes. The first peak of E = 367 μV/m and B = 19.2 pT at 07:04:11.19 UTC (61.79°N, 145.295°W, as projected to the D region along a magnetic field line) occurs at a distance of 73 km. The second peak of E = 366 μV/m and B = 5.8 pT at 07:04:13.86 UTC (61.94°N, 145.81°W) occurs at a distance of 61 km. The frequencies at which the peaks occur are 605 Hz and 1172 Hz respectively. It should be noted that the peak E field amplitudes are observed before the satellite reaches the closest point to the HAARP field line (07:04:19.59 UTC, 62.26°N, 146.04°W) indicating that the region of maximum signal is slightly displaced southward. This observation qualitatively confirms AUREOL-3 measurements over Tromso HF heater [*Lefeuvre et al.*, 1985] of a 3° southward displacement at 1900 km altitude (d = 200 km). The B field intensity on the ground was ~0.1 pT during the E field peaks on DEMETER, which is lower than the average values observed at Chistochina at this frequency. The electron density measured on the satellite was $4 \cdot 10^3$ cm^{-3}. The other 2 components of E and B up to 1250 Hz were also measured on DEMETER at levels comparable with components shown in Figures 2 and 3. It should also be noted that the proton gyrofrequency on DEMETER was f_{c_H} = 636 Hz which is close to the frequency of the first maximum. However, Oxygen was the dominant ion at the time of the observations ($N_{O^+} = 4 \cdot 10^3$ cm^{-3}, $N_{H^+} < 10$ cm^{-3}) so that Hydrogen influence on waves propagation should be minimal. Also, if the first maximum was due to the decrease in group velocity as the waves approach the point of absorption, the polarization of these waves should be circular left-hand, but it was calculated using the method of *Santolik et al.* [2006] that the waves in the maximum have close to linear polarization (the ratio of the axes of the polarization ellipse is from 0 to 0.2). The waves in the second maximum exhibit circular right hand polarization as expected for frequencies above f_{c_H}. The calculation of wave normal angle using the method of *Santolik et al.* [2006] gives $\theta \simeq 110°–150°$ below f_{c_H} and $\theta \simeq 90°–120°$ above f_{c_H} (θ is an angle between directions of Earth's magnetic field and wave vector).

[13] For another well-situated DEMETER pass on 26 February 2007 (Figure 4) the second transmission pattern was used (Table 1). The pattern basically represents two

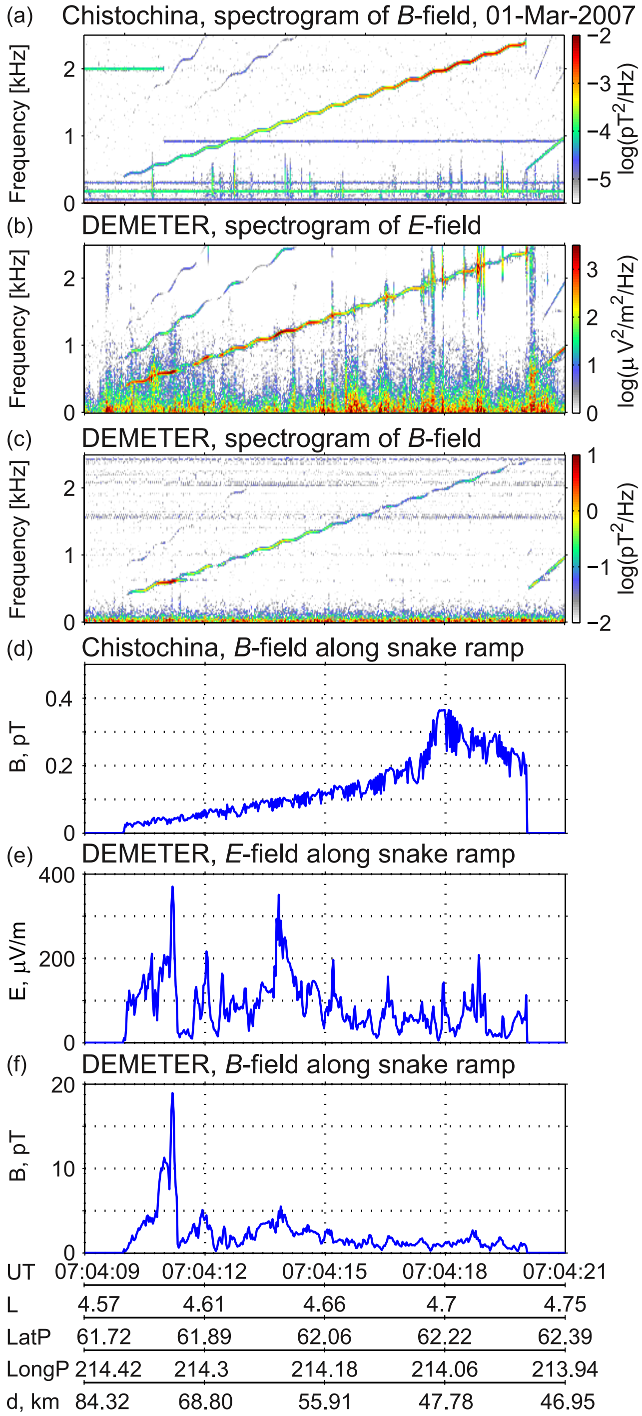

Figure 3. Comparison of ground and DEMETER E and B fields for the closest part of the pass on 1 March 2007: (a–c) Magnified version of the spectrograms shown in Figure 2 and (d–f) linear plots of field magnitudes calculated along main harmonic of the snake ramp from corresponding field spectrograms on the top.

intermittent sequences of 1-s tones with 4-s periodicity, eliminating the frequency dependence uncertainty and allowing the direct measurement of the spatial profile of HAARP-induced ELF signal. In Figure 4a the spectrogram of E field for the closest part of the pass is shown. Figures 4b and 4c show the 1-s average of a horizontal component of the E field on DEMETER filtered in a 4.9 Hz band around two ELF frequencies of HAARP modulation. The corresponding satellite track is plotted in Figure 4d. The data indicate that the signal is detectable from about 900 km south of HAARP to about 300 km north. The region of the strongest signal is once again slightly displaced southward; however we can see that the closest point to the HAARP field line is also southward of HAARP as shown by an arrow. Another factor which may contribute to the observed southward displacement of the amplitude peak is the radiation pattern of the ionospheric ELF source currents. If the source current is crudely represented as an east–west dipole antenna [*Payne et al.*, 2007], then pattern nulls should occur in the east–west direction at the altitude of the source, so that the satellite may actually observe the decrease of the field westward from HAARP. The region of the strongest signal ranges from $\simeq$200 km north to $\simeq$300 km south of the HAARP field line as marked by dashed lines. The magnitude of the strongest pulse at 1111 Hz was E = 40 μV/m, which is an order of magnitude lower than that for the 1 March 2007 case. It is likely that in this case the satellite just did not reach the region of the highest possible field since the closest point is at a distance d = 122 km. On the other hand the signal propagated further away in the Earth-ionosphere waveguide, and signal at f = 1111 Hz is detected as far as $d\simeq$900 km south, while at f = 2011 Hz the longest distance was d = 831 km. The northern part of the pass exhibited higher natural noise and detection was more problematic because of lower signal to noise ratio. The magnetic field on DEMETER is above noise level just for some closest pulses of 1111 Hz with amplitude of the closest pulse $\simeq$ 1 pT. For comparison, the measurement at Chistochina showed $B \simeq 0.25$ pT, and for this period the Kp index was 2^- and the AE index was 24 nT. The calculation of wave normal angle for these close pulses gives $\theta = 100°$.

[14] The case on 26 February 2007 is very typical in terms of signal levels and the extent of the maximum observed at such distances in nighttime conditions. Among four other successful detections during the campaign there were two more nighttime passes and the maximum E field was of the order of 10 μV/m within $d \simeq$ 200–300 km. The remaining two passes were during daytime with signals detected just within $d \simeq$ 200–300 km and magnitudes of about 1 μV/m, which can be attributed to increased ionospheric absorption for daytime conditions.

4. Discussion

[15] DEMETER observations of HAARP-induced ELF signals over long distances suggest that there exist three distinct spatial regions (Figure 1), classified simply on the basis of signal strength and distance of the DEMETER magnetic footprint at 75-km from the HAARP heated spot.

[16] The first and relatively large region is characterized by relatively low field magnitudes, extending from $d \simeq$ 200–300 to $d \simeq$ 900 km (Figure 4). Within this region the signal observed is likely that which is launched from the source region into the Earth-ionosphere waveguide, within which it propagates while continually leaking upward and reaching the satellite as a whistler mode wave propagating close to the zenith direction. The outer boundary of this

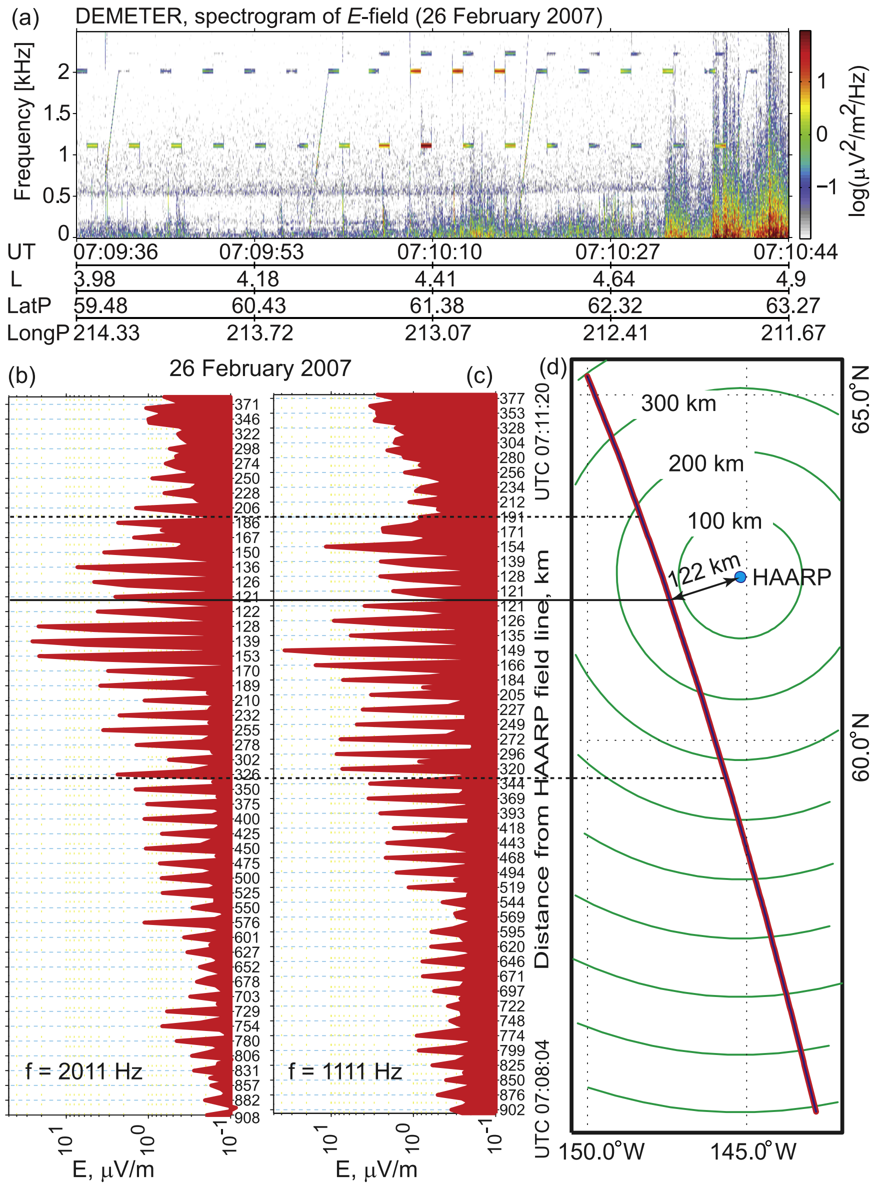

Figure 4. DEMETER pass on 26 February 2007. (a) Spectrogram of a horizontal component of *E* field on DEMETER. (b) One-second average of *E* field on DEMETER filtered over narrow band ($\Delta f = 4.9$ Hz) around 2011 Hz. (c) The same around 1111 Hz. (d) A map showing projection along the Earth's magnetic field lines of the corresponding satellite pass onto the horizontal plane at the altitude of the source (75 km).

region may substantially differ from day to day and depends on the magnitude of the originally launched signal and its attenuation within the waveguide and during trans-ionospheric transmission to satellite altitudes.

[17] The second region of relatively higher fields extends to $d \simeq 200-300$ km. DEMETER encounters this region on 26 February 2007 at its closest position to HAARP and on 1 March 2007 when the signal is first detectable, but before the highest field magnitudes are measured. This region was also seen during four other passes not considered here in detail. The region is slightly displaced southward with respect to the field line of the source in both cases reported herein in detail and in prior observations [*Lefeuvre et al.*, 1985]. This region is likely characterized by the fact that the waves arriving at the satellite without reflection from the ground dominate over those which are at least once reflected from the ground. Direct waves are stronger in amplitude but fall off faster with the distance from the source than waves propagating in the waveguide (as schematically represented in Figure 1). Thus, the outer boundary of this region can be defined as the location at which the direct waves become weak enough to be comparable with those leaking upward from the waveguide.

[18] The third region is characterized by extremely high fields, has a spatial extent of the order of 10 km in radius, and is located within $d < 100$ km from the source field line. It thus appears that there exists a cylindrical column (with radius of 10–20 km) of the waves emanating from the

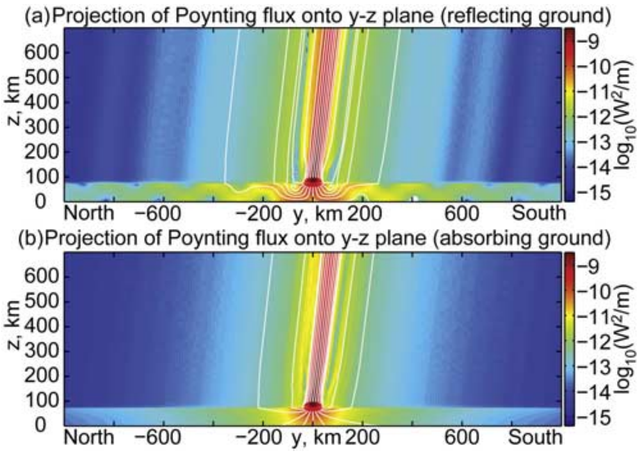

Figure 5. Projection of Poynting vector $\vec{S}$ onto plane y-z calculated using model of *Lehtinen and Inan* [2008]. Background color represents magnitude of the projection $\sqrt{S_y^2 + S_z^2}$; white lines are streamlines of the projection coming from a region around the source. (a) A case with realistic reflecting boundary conditions at the surface of the ground. (b) Same case as shown in Figure 5a, with the exception that the ground is now considered to be totally absorbing.

source region (i.e., the HF heated region at 75 km) propagating upward along the magnetic field lines or slightly displaced from the field lines. The maximum lateral distance between the magnetic footprint of the satellite and the center of the source within which such column can occur is approximately 100 km, because in no pass beyond this distance have high fields ever been observed. A column radius of 10–20 km is a rough estimation based on the width of the first maximum at the E = 100 μV/m level, or alternatively on the distance between the two relative maxima for the pass on 1 March 2007. In addition, it may turn out that such a column is actually not displaced from the field line of the source and therefore is larger in radius so that we observe only a part of the column. Our review of the literature suggests that up to now this region (i.e., the column) has been traversed by a spacecraft only once before when an HF heater was modulated with ELF/VLF frequencies (ISIS 1 on 9 December 1981 [*James et al.*, 1984]). DEMETER observations of extremely high fields in situ and moderate fields on the ground as reported herein provide the support for the validity of ISIS 1 observations. The results of EXOS-D (Akebono) satellite measurements over HIPAS [*Kimura et al.*, 1991] and over Tromso heater [*Kimura et al.*, 1994] as well as DEMETER measurements on 1 March 2007 over HIPAS and over HAARP on 26 February and during other experiments did not exhibit such high fields probably because the satellite trajectories simply missed these small columnar regions in those cases. The observed double maxima in E field may be due to irregular field distribution inside the column or variations in time. This double maxima behavior is not likely to be due to frequency dependence of generation or propagation, since the raypaths of whistler waves at these frequencies are unlikely to be separated by the distance of $\simeq$20 km at 670-km altitude due to refractive index dependence on frequency. On the other hand, the scattering of waves on the density irregularities in the heated region can lead to the decrease of signal inside the parts of the cylindrical column and explain the random variations of the E and B amplitudes between the two maxima.

[19] One possible explanation of the propagation of ELF waves to the satellite altitude in regions 2 and 3 is put forth by *James et al.* [1984, Figure 9] using ray tracing; they showed that rays could be spread within the cone of 20° if the starting wave normal angle at the source is within the cone of 65°. However, consideration of the dispersion diagram for whistler-mode waves and the size of real source region, i.e., the heated spot [*Lehtinen and Inan*, 2008, Figure 3], shows that the distribution of initial wave normal angles is much narrower than 65°, thus leading to less spread of the wave power going upward.

[20] A realistic full-wave model of ELF/VLF radiation by modulation of the electrojet with consideration of the finite size of the source region has recently been developed by *Lehtinen and Inan* [2008]. An example of a model run is presented in Figure 5, which shows the magnitude of the projection of the Poynting vector $\vec{S}$ onto a north–south vertical plane passing through the source. White lines represent the streamlines of the projection calculated for specific initial points around the source. The simulation in Figure 5a is performed with realistic boundary conditions of perfectly conducting ground, while in Figure 5b boundary conditions on the ground were assumed to be totally absorbing. Figures 5a and 5b clearly show the existence of an intense upgoing column of ELF/VLF radiation excited by an HF heater with the column size equal to the heated spot. The column is basically not influenced by the existence of the ground. In the second region just fields configuration is changed slightly by the ground presence, while the power delivered to the satellite altitude is mostly the same. The most interesting observation concerns the way by which waves reach the satellite in region two. At first ELF waves propagate from the source as surface waves at the ionospheric boundary (e.g., where the gradient of electron density in D region is present), and then part of the wave energy penetrates into the ionosphere where the waves propagate close to the magnetic field lines. Therefore, the observations on DEMETER in the second region are almost independent of the presence of the ground. On the other hand, if in Figure 5 we look, for example, at the distance of $d \simeq 650$ km to the south of the source we clearly see the difference between the projections of the Poynting flux in the Figure 5a and Figure 5b cases. It is worth noting that the difference in the field strength in region 1 with and without ground as it is modeled by *Lehtinen and Inan* [2008] is relatively small.

[21] It should be mentioned that there was one more observation of strong waves generated by the Tromso HF heater [*Robinson et al.*, 2000] on the FAST spacecraft at an altitude of 2550 km. Later it was shown that the spacecraft was within d = 15 km during this detection [*Wright et al.*, 2003]. However, the modulation frequency in that case was in ULF range, 3 Hz, and therefore the comparison of guiding properties and amplitudes may not be appropriate. The guiding of ULF waves along B_0 would be expected if only the Alfven mode is excited, however if the magnetosonic mode is excited, it will not be guided along magnetic

field lines as its refractive index is isotropic. The guidance and the existence of the column for low altitudes for ELF waves is ensured not only by the refractive index of whistler mode but also by narrow initial distribution of wave vectors (see discussion by *Lehtinen and Inan* [2008, section 3.1]). For ULF waves, on the other hand, the ratio of wavelength to the size of the source is more than 100 making the source effectively a point source with a wide range of initial wave normal angles.

[22] Finally, we make a simple comparison of power levels of present (1 March 2007) and previous results in the same way as it was done by [*Kimura et al.*, 1991]. A wave magnetic field of 0.1 pT measured at Chistochina gives an ionospheric current at the distance of 100 km $I = 2\pi rB/\mu_0 \simeq 0.05$ A. According to [*James et al.*, 1984] a dipole current of 1 A results in the peak vertical energy flux of 10^{-10} W/m^2 at altitude of ISIS 1. Scaling down this value by calculated current we get the flux $\propto I^2$ equal to $2.5 \cdot 10^{-13}$ W/m^2. Moreover, taking into account the fact that the energy flux will be a little higher at DEMETER if the wave energy in the same geomagnetic flux tube is kept constant we get $3 \cdot 10^{-13}$ W/m^2. For comparison, the energy flux observed by DEMETER for the first discussed maximum is $4 \cdot 10^{-9}$ W/m^2 and for a wider region around the maximum ($r \simeq 10$ km) with average $E = 100$ μV/m and $B = 5$ pT we get $3 \cdot 10^{-10}$ W/m^2. It is clear that older models underestimate the flux inside the column while the full wave model [*Lehtinen and Inan*, 2008, Figure 4] predicts the peak value of $1.6 \cdot 10^{-9}$ W/m^2 at the altitude of DEMETER.

5. Summary

[23] DEMETER spacecraft observations of ELF signals induced by the recently upgraded HAARP ionospheric heater suggest that the ELF signal illumination region can be divided into three distinctive regions. In the first region ranging from $d \simeq 200-300$ km to at least 900 km the signal observed is that which propagates in the Earth-ionosphere waveguide and leaks upward into the magnetosphere. In the second region within $d \simeq 200-300$ km of the HAARP field line, signal observed is that which propagates from the D region source to the satellite without reflection from ground. The third region of $\sim$10–20 km in radius which is seen at an altitude of 75 km within $d \sim 100$ km from the HAARP field line is characterized by extremely high signal ($E = 367$ μV/m, $B = 19.2$ pT) accounting for the previously noted discrepancy in the electrojet current calculations based on in situ versus ground measurements. These observations suggest the presence of a cylindrical column of ELF radiation close to the field line as recently put forth by *Lehtinen and Inan* [2008] via modeling.

[24] **Acknowledgments.** The Stanford portion of this work was supported by the Defense Advanced Research Projects Agency (DARPA) and the High Frequency Active Auroral Research Program (HAARP) under ONR grants N00014-05-1-0854 to Stanford University. The authors thank J. J. Berthelier, who provided us with data from the electric field instrument on DEMETER, and O. Santolik, who made his algorithms for wave analysis widely available over the Internet.

[25] Amitava Bhattacharjee thanks Michael Rietveld and Michael Starks for their assistance in evaluating this paper.

References

Getmantsev, C. G., N. A. Zuikov, D. S. Kotik, L. F. Mironenko, N. A. Mityakov, V. O. Rapoport, Y. A. Sazonov, V. Y. Trakhtengerts, and V. Y. Eidman (1974), Combination frequencies in the interaction between high-power short-wave radiation and ionospheric plasma, *JETP Lett.*, Engl. Transl., *20*, 101–102.

Helliwell, R. A., J. P. Katsufrakis, T. F. Bell, and R. Raghuram (1975), VLF line radiation in the Earth's magnetosphere and its association with power system radiation, *J. Geophys. Res.*, *80*, 4249–4258.

James, H. G., R. L. Dowden, M. T. Rietveld, P. Stubbe, and H. Kopka (1984), Simultaneous observations of ELF waves from an artificially modulated auroral electrojet in space and on the ground, *J. Geophys. Res.*, *89*, 1655–1666.

Kapustin, I. N., R. A. Pertsovsky, A. N. Vasil'ev, V. S. Smirnov, O. M. Raspopov, L. E. Solov'eva, A. A. Ul'yachenko, A. A. Arykov, and N. V. Galakhova (1977), Generation of radiation at combination frequencies in the region of the auroral electrojet, *JETP Lett.*, Engl. Transl., *25*(5), 248–251.

Kennedy, E. J., and P. Kossey (2002), Description of the HAARP Gakona facility with some results from recent research, paper presented at XXVIIth General Assembly of URSI, Union Radio Sci. Int., Maastricht, Netherlands, 17–24 Aug.

Kimura, I., A. Wong, B. Chouinard, T. Okada, M. McCarrick, I. Nagano, K. Hashimoto, R. Wuerker, M. Yamamoto, and K. Ishida (1991), Satellite and ground observations of HIPAS VLF modulation, *Geophys. Res. Lett.*, *18*, 309–312.

Kimura, I., P. Stubbe, M. T. Rietveld, R. Barr, K. Ishida, Y. Kasahara, S. Yagitani, and I. Nagano (1994), Collaborative experiments by Akebono satellite, Tromso ionospheric heater, and European incoherent scatter radar, *Radio Sci.*, *29*, 23–37.

Lefeuvre, F. et al. (1985), Detection from AUREOL-3 of the modulation of auroral electrojet by HF-heating from ELF signals in the upper ionosphere above Tromsoe, in *Results of the Arcad 3 Project and of Recent Programmes in Magnetospheric and Ionospheric Physics Toulouse*, vol. 84, pp. 609–619, Cepadues Ed., Toulouse, France.

Lehtinen, N. G., and U. S. Inan (2008), Radiation of ELF/VLF waves by harmonically varying currents into a stratified ionosphere with application to radiation by a modulated electrojet, *J. Geophys. Res.*, *113*, A06301, doi:10.1029/2007JA012911.

Moore, R. C., U. S. Inan, and T. F. Bell (2006), Observations of amplitude saturation in ELF/VLF wave generation by modulated HF heating of the auroral electrojet, *Geophys. Res. Lett.*, *33*, L12106, doi:10.1029/2006GL025934.

Parrot, M., (Ed.) (2006), Special Issue: First Results of the DEMETER Micro-Satellite, *Planet. Space Sci.*, *54*(5), 411–558.

Payne, J. A., U. S. Inan, F. R. Foust, T. W. Chevalier, and T. F. Bell (2007), HF modulated ionospheric currents, *Geophys. Res. Lett.*, *34*, L23101, doi:10.1029/2007GL031724.

Platino, M., U. S. Inan, T. F. Bell, M. Parrot, and E. J. Kennedy (2006), DEMETER observations of ELF waves injected with the HAARP HF transmitter, *Geophys. Res. Lett.*, *33*, L16101, doi:10.1029/2006GL026462.

Rietveld, M. T., P. Stubbe, and H. Kopka (1989), On the frequency dependence of ELF/VLF waves produced by modulated ionospheric heating, *Radio Sci.*, *24*, 270–278.

Robinson, T. R., et al. (2000), FAST observations of ULF waves injected into the magnetosphere by means of modulated RF heating of the auroral electrojet, *Geophys. Res. Lett.*, *27*(19), 3165–3168.

Santolik, O., F. Nemec, M. Parrot, D. Lagoutte, L. Madrias, and J. J. Berthelier (2006), Analysis methods for multi-component wave measurements on board the DEMETER spacecraft, *Planet. Space Sci.*, *54*(5), 512–527, doi:10.1016/j.pss.2005.10.020.

Stubbe, P., H. Kopka, M. T. Rietveld, and R. L. Dowden (1982), ELF and VLF generation by modulated HF heating of the current carrying lower ionosphere, *J. Atmos. Terr. Phys.*, *44*, 1123–1135.

Wright, D. M., et al. (2003), Detection of artificially generated ULF waves by the FAST spacecraft and its application to the "tagging" of narrow flux tubes, *J. Geophys. Res.*, *108*(A2), 1090, doi:10.1029/2002JA009483.

T. F. Bell, U. S. Inan, N. G. Lehtinen, and D. Piddyachiy, STAR Laboratory, Stanford University, Packard Building, Room 351, 350 Serra Mall, Stanford, CA 94305, USA. (depi@stanford.edu)

M. Parrot, Laboratoire de Physique et Chimie de l'Environnement, CNRS, 3A Avenue de la Recherche Scientifique, F-45071 Orléans, France.